ARTICLE

Check for updates

Journal of
Sensor Science and Technology

The Korean Sensors Society

Common-Mode Choke for Common-Mode and Differential-Mode Noise Suppression in Low-Power AC-to-DC Power Converters in Sensor Power Modules

Jong-Hae Kim[1], Young-Woo Kim[2], Jae-Sun Won[3], Ku-Yong Kim[4], Do Kyung Lee[5,+], and Young-Soo Sohn[6,+]

[1]*Department of Electrical Engineering, Daegu Catholic University, 13-13 Hayangro, Hayang-eup, Gyeongsan, 38430, Republic of Korea*
[2]*Department of Electrical Engineering, Korea National University of Transportation, 50 Daehak-ro, Daesowon-myeon, Chungju, 27469, Republic of Korea*
[3]*MLCC Design Lab of the Component Business Unit, Samsung Electro-Mechanics Co. Ltd, 150 Maeyeong-ro, Yeongtong-gu, Suwon, 16674, Republic of Korea*
[4]*MDM Daegu Design Center, 32 Seongseogongdan-ro, Dalseo-gu, Daegu, 42714, Republic of Korea*
[5]*Department of Advanced Materials Science and Chemical Engineering, Daegu Catholic University, 13-13 Hayangro, Hayang-eup, Gyeongsan, 38430, Republic of Korea*
[6]*College of Francisco, Daegu Catholic University, 13-13 Hayangro, Hayang-eup, Gyeongsan, 38430, Republic of Korea*

Cite This: *J. Sens. Sci. Technol. Vol. 34, No. 4 (2025) 261-271*

https://doi.org/10.46670/JSST.2025.34.4.261

ABSTRACT: This paper proposes a common-mode (CM) choke with an asymmetrical CM winding and differential-mode (DM) noise suppression for low-power AC-to-DC power converters in sensor power modules. For a conventional CM choke with symmetrical winding, the CM and DM noises are also attenuated by the magnetizing inductance (L_M) and very small leakage inductance (L_k) owing to the higher coupling factor, respectively, of the CM choke. However, because the number of turns is limited according to the shape and size of the CM choke, determining the proper L_k to eliminate the DM noise thoroughly is difficult. Therefore, a bulky CM choke is required for a larger L_k. Typically, another DM choke is used for DM noise attenuation. Thus, the cost and size of the electromagnetic interference (EMI) filters for use with a conventional CM choke can increase. To solve these problems, we propose a CM choke with an asymmetrical winding. In contrast to the conventional CM choke with a symmetrical winding, the L_m of the CM choke with an asymmetrical winding can suppress both CM and DM noises. Therefore, the proposed CM choke can effectively attenuate CM and DM noises with fewer and smaller turns. This method can be applied to all types of AC-to-DC power converters of sensor power modules that use two- or three-stage systems. To confirm the validity and superiority of the proposed CM choke, this paper compares the total, DM, and CM noise characteristics between conventional and proposed CM chokes. Finally, a practical approach to designing EMI filters and the design procedures are also addressed.

KEYWORDS: *EMI filter, Conducted EMI, Asymmetrical winding CM choke, CM and DM noise attenuation, Sensor power modules*

1. INTRODUCTION

Recently, most power conversion systems use a switch-mode power supply (SMPS), which satisfies the requirements of high efficiency, high power density, and high reliability. The flyback converter is one of the most commonly used topologies, particularly in low-power AC-to-DC converters such as those in TVs, smartphone chargers, laptop adapters, sensor power modules, and set-top boxes. The high-frequency switching operation of these systems is the main source of high-frequency conducted electromagnetic interference (EMI) noise owing to the fast switching currents di/dt and voltages dv/dt. In particular, sensor power modules used with low-power AC-to-DC converters must be designed carefully to minimize EMI noise, which can disrupt sensor operation [1-4]. Therefore, EMI filters have been widely used for many years to suppress high-frequency conducted EMI noise in power electronic applications [5-9]. Because EMI noise can

[+]Corresponding author: dokyung@cu.ac.kr, sohnys@cu.ac.kr
Received : Jun. 29, 2025, Revised : Jul. 2, 2025, Accepted : Jul. 5, 2025

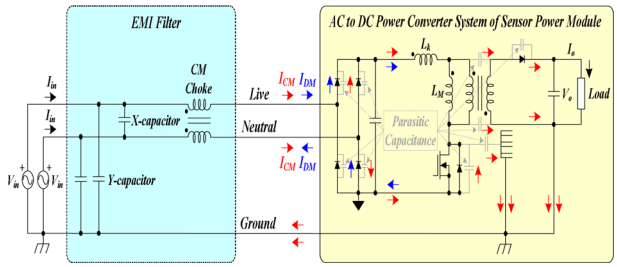

Fig. 1. CM and DM noise currents in AC-to-DC power converter of sensor power module with a flyback DC-to-DC converter.

affect other power electronic systems connected to the same line, CISPR, an organization affiliated with the International Electrical Committee (IEC), establishes noise limits at certain levels. The CISPR limits concern the conducted and radiated emissions of devices, where the conducted emissions are caused by currents passing through the AC power cord of the unit [10]. Therefore, EMI filters have been largely used for AC-to-DC converters, DC-to-DC converters, etc., particularly in power electronics, to attenuate switching noise and satisfy EMI standards. EMI noise is traditionally categorized into differential-mode (DM) and common-mode (CM) currents, particularly in low-power AC-to-DC power converters of sensor power modules with flyback DC-to-DC converters, as shown in Fig. 1.

While DM noise is caused by the noise current flowing within the power delivery path, CM noise is caused by the noise current flowing between the chassis ground and power circuit [11]. CM and DM chokes are required to suppress these types of noises. Generally, a CM choke includes a very small leakage inductance (L_k) and a large magnetizing inductance (L_M) because the coupling coefficient (K) is less than 1.0, where L_M and L_k serve as CM and DM chokes, respectively. However, if the level of DM noise is high in the frequency range below 1 MHz, a very small L_k cannot attenuate it to a suitable level. Therefore, several serially connected CM chokes, a CM choke with a greater number of turns for large L_k, or an additional large DM choke have been used. However, these conventional methods not only increase the filter size and cost of production but also deteriorate the power conversion efficiency. To overcome these limitations, several researchers have analyzed an integrated EMI choke for DM and CM noise suppression and a CM choke with an asymmetric winding. However, to the best of our knowledge, the analysis results have not been clearly described [12,13]. Therefore, this paper proposes a CM choke with an asymmetrical winding, in which the turns ratio between the primary and secondary windings are not equal, and analyzes it qualitatively and in more detail compared with earlier research. The main concept of the proposed CM choke with an asymmetrical winding is that is uses both L_k and L_M to attenuate the CM and DM noises simultaneously. The proposed method simplifies the construction of an EMI filter without requiring additional components. To verify the feasibility and superiority of the proposed CM choke with an asymmetrical winding, we compare the overall, DM, and CM noise characteristics of conventional and proposed CM chokes. Finally, a practical approach for designing an EMI filter is presented.

2. CM AND DM NOISE MODELING OF THE PROPOSED CM CHOKE WITH AN ASYMMETRICAL WINDING

Because the characteristics of CM and DM noises differ, the parasitic elements related to CM noise also differ from those of DM noise. The CM and DM noise models of a conventional CM choke are shown in Figs. 2 (a) and 2 (b), respectively. The two windings (L_1 and L_2), with the same number of turns on the primary and secondary windings ($N_1 = N_2$), serve as conventional CM choke windings, where N_1 is the number of turns on the primary side, and N_2 is the number of turns on the secondary side of a conventional CM choke. The equivalent CM and DM impedances of a conventional CM choke are used to estimate the CM and DM noise models. The formal equations can be generally expressed as Eqs. (1) and (2) to analyze the equivalent CM and DM impedances of a conventional CM choke [14-16].

$$\begin{cases} V_{CM1} = sL_1 I_{CM1} + sM_{12} I_{CM2} \\ V_{CM2} = sL_2 I_{CM2} + sM_{21} I_{CM1} \end{cases} \quad (1)$$

$$\begin{cases} V_{DM1} = sL_1 I_{DM1} - sM_{12} I_{DM2} \\ V_{DM2} = sL_2 I_{DM2} - sM_{21} I_{DM1} \end{cases} \quad (2)$$

where V_{CMi} and I_{CMi} ($i = 1, 2$) are the voltage of L_i and CM noise current, respectively, as shown in Fig. 2 (a). V_{DMi} and I_{DMi} ($i = 1, 2$) are the voltage of L_i and DM noise current, respectively, as shown in Fig. 2 (b). M_{ij} (i, $j = 1, 2$, $i \neq j$) represents the mutual inductance between the primary and secondary windings. The mutual inductances of the primary and secondary windings to the secondary and primary windings are defined as M_{12} and M_{21}, respectively, which have the same values; therefore, $M_{12} = M_{21} = M$. I_{CM1} and I_{CM2} currents in the live and neutral lines theoretically have the same magnitude when considering only CM noise currents; therefore, $I_{CM1} = I_{CM2} = I_{CM}/2$. I_{DM1} and I_{DM2}, currents in the live and neutral lines, have theoretical currents flowing in opposite directions but have the same magnitude when considering only DM noise currents; therefore, $I_{DM1} = I_{DM2} = I_{DM}$. As shown in Fig. 2 (b), according to Kirchhoff's voltage and current laws, V_{DM} can be expressed as the sum of V_{DM1} and V_{DM2}. For

simplicity, the mutual inductance between the primary and secondary windings can be determined using transformer theory. This is because the primary and secondary windings are wound on the same toroidal core and are perfectly coupled; therefore, K is 1.0. In other words, when the inductances of the two windings are equal, $L_1 = L_2$, the mutual inductance that exists between the two windings will equal the value of a single winding, as the square root of two equal values is the same as a single value, as shown in Eq. (3).

$$M = K\sqrt{L_1 L_2}(\because K = 1) = \frac{N_2}{N_1}L_1 = \frac{N_1}{N_2}L_2 \tag{3}$$

where, as described above, if N_1 is equal to N_2, M, which is the mutual inductance between the two windings, can be expressed as $M = L_1 = L_2 = L_M$ based on Eq. (3).

Using Eqs. (1)–(3), the equivalent CM and DM impedances (Z_{CM} and Z_{DM}) of a conventional CM choke can be expressed as Eqs. (4) and (5), respectively.

$$\begin{cases} Z_{CM1} = \frac{V_{CM1}}{I_{CM1}} = s(L_M + M) = 2sL_M \\ Z_{CM2} = \frac{V_{CM2}}{I_{CM2}} = s(L_M + M) = 2sL_M \end{cases} \tag{4}$$

$$\begin{cases} Z_{DM1} = \frac{V_{DM1}}{I_{DM1}} = s(L_M - M) = 0 \\ Z_{DM2} = \frac{V_{DM2}}{I_{DM2}} = s(L_M - M) = 0 \end{cases} \tag{5}$$

where Z_{CM1} and Z_{CM2} are the equivalent CM impedances of a conventional CM choke, which have the same values and attenuate the CM noise currents; thus, $Z_{CM1} = Z_{CM2} = Z_{CM}$. Z_{DM1} and Z_{DM2} are the equivalent CM impedances of a conventional CM choke and have the same value; therefore, $Z_{DM1} = Z_{DM2} = Z_{DM}$. However, as shown in Eq. (3), because the mutual inductance (M) is theoretically equal to L_1 and L_2, Z_{DM1} and Z_{DM2} become zero, and for the same values, Z_{DM1} and Z_{DM2} cannot attenuate the DM noise currents. As stated above, Z_{DM} can be expressed as the sum of Z_{DM1} and Z_{DM2} because V_{DM} is the sum of V_{DM1} and V_{DM2}.

Based on Eqs. (4) and (5), the CM and DM inductances (L_{CM} and L_{DM}) involved in the CM and DM impedances of a conventional CM choke can be expressed as Eqs. (6) and (7), respectively.

$$L_{CM} = \frac{V_{CM1}}{I_{CM}} = \frac{V_{CM2}}{I_{CM}} = L_M \tag{6}$$

$$L_{DM} = \frac{V_{DM}}{I_{DM}} = \left(\frac{V_{DM1}}{I_{DM1}} + \frac{V_{DM2}}{I_{DM2}}\right) = 0 \tag{7}$$

As shown in Eqs. (6) and (7), when the K is perfectly coupled, a conventional CM choke can only attenuate CM noise.

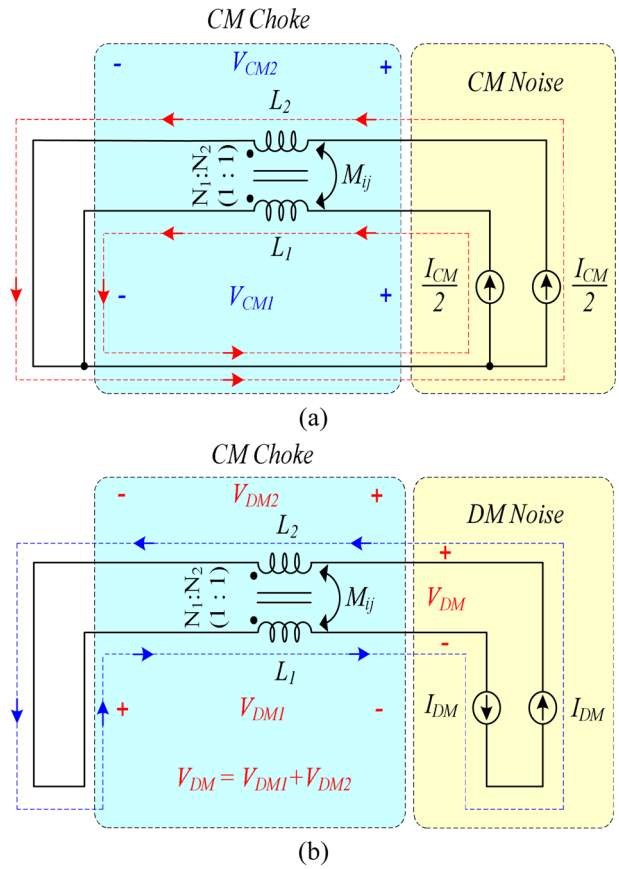

Fig. 2. CM and DM noise modeling of conventional CM choke: (a) CM noise modeling, (b) DM noise modeling.

However, generally, a conventional CM choke includes a very small L_k, as well as a large L_M because it is not tightly coupled, with a K of less than 1.0, where L_M and L_k serve as CM and DM chokes, respectively. The equivalent CM and DM impedances of a conventional CM choke, considering L_M and L_k, are used to estimate the CM and DM noise models. The formal equations, including L_M, L_k, and mutual inductances (M_{21} and M_{12}), can generally be expressed as Eqs. (8) and (9) to analyze the equivalent CM and DM impedances of a conventional CM choke.

$$\begin{cases} V_{CM1} = s(L_{21} + L_{1k})I_{CM1} + sM_{12}I_{CM2} \\ V_{CM2} = s(L_{12} + L_{2k})I_{CM2} + sM_{21}I_{CM1} \end{cases} \tag{8}$$

$$\begin{cases} V_{DM1} = s(L_{21} + L_{1k})I_{DM1} - sM_{12}I_{DM2} \\ V_{DM2} = s(L_{12} + L_{2k})I_{DM2} - sM_{21}I_{DM1} \end{cases} \tag{9}$$

where the self-inductances (L_1 and L_2) between the two windings are the sum of the magnetizing inductances (L_{21} and L_{12}) and the leakage inductances (L_{1k} and L_{2k}), respectively. L_{1k} and L_{2k} are the leakage inductances of the self-inductances, which have the same value; therefore, $L_{1k} = L_{2k} = L_k$. The

mutual inductances (M_{12} and M_{21}) of the primary and secondary windings to the secondary and primary windings are determined by the control factors of the coupling coefficients (K_{12} and K_{21}), the number of turns on the primary and secondary windings (N_1 and N_2), self-inductances (L_1 and L_2), and magnetizing inductances (L_{21} and L_{12}). Therefore, if K of the two windings is less than 1, M_{12} and M_{21} can be expressed by Eqs. (10) and (11). As stated above, I_{CM1} and I_{CM2} in the live and neutral lines also theoretically have the same magnitude when considering only CM noise currents; therefore, $I_{CM1} = I_{CM2} = I_{CM}/2$. I_{DM1} and I_{DM2} in the live and neutral lines have theoretical currents flowing in opposite directions but have the same magnitude when considering only DM noise currents; therefore, $I_{DM1} = I_{DM2} = I_{DM}$.

$$M_{21} = K_{21}\sqrt{L_1 L_2} = \frac{N_2}{N_1}K_{21}L_1 = \frac{N_2}{N_1}L_{21} \tag{10}$$

$$M_{12} = K_{12}\sqrt{L_1 L_2} = \frac{N_1}{N_2}K_{12}L_2 = \frac{N_1}{N_2}L_{12} \tag{11}$$

where, as shown in Eqs. (10) and (11) if N_1 and K_{21} are equal to N_2 and K_{12}, M_{12} and M_{21} are the mutual inductances of the primary and secondary windings to the secondary and primary windings, respectively, which have the same values: $M_{12} = M_{21} = L_{21} = L_{12} = L_M$ [17,18].

As described above, using Eqs. (8)–(11), the equivalent CM and DM impedances of a conventional CM choke can be expressed as Eqs. (12) and (13).

$$\begin{cases} Z_{CM1} = \frac{V_{CM1}}{I_{CM1}} = 2sL_M + L_k \\ Z_{CM2} = \frac{V_{CM2}}{I_{CM2}} = 2sL_M + L_k \end{cases} \tag{12}$$

$$\begin{cases} Z_{DM1} = \frac{V_{DM1}}{I_{DM1}} = L_k \\ Z_{DM2} = \frac{V_{DM2}}{I_{DM2}} = L_k \end{cases} \tag{13}$$

Fig. 3 shows the CM and DM noise current flows of a conventional CM choke, considering L_M and L_k.

As shown in Fig. 3, because the CM noise currents in the live and neutral lines flow in the same direction, the L_M of a traditional CM choke participates in attenuating the CM noise. In contrast, because the DM noise currents in the live and neutral lines flow in opposite directions, the L_k contributes to the attenuation of the DM noise.

Using Eqs. (12) and (13), the CM and DM inductances (L_{CM} and L_{DM}) involved in the CM and DM impedances of a conventional CM choke, respectively, can be expressed as Eqs. (14) and (15).

$$L_{CM} = \frac{V_{CM1}}{I_{CM}} = \frac{V_{CM2}}{I_{CM}} = s\left(\frac{2L_M + L_k}{2}\right) \cong L_M \tag{14}$$

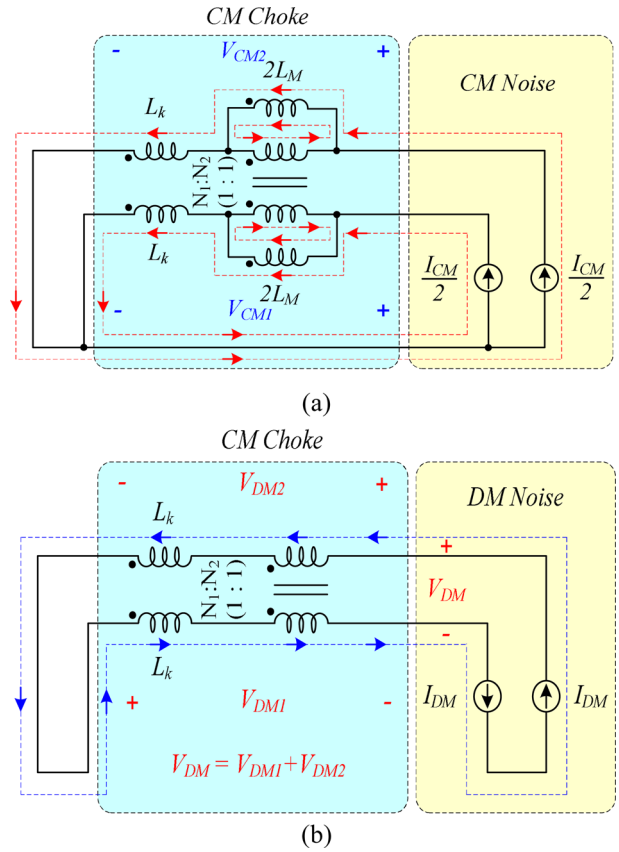

Fig. 3. CM choke CM and DM noise current flows of a conventional CM choke considering the magnetizing inductance (L_M) and leakage inductance (L_k); (a) CM noise current, (b) DM noise current.

$$L_{DM} = \frac{V_{DM}}{I_{DM}} = \left(\frac{V_{DM1}}{I_{DM1}} + \frac{V_{DM2}}{I_{DM2}}\right) = 2L_k \tag{15}$$

where Eqs. (14) and (15) are the simplified equivalent inductances of the CM and DM inductances (L_{CM} and L_{DM}) considering L_M and L_k because L_k of the conventional CM choke is much smaller than its L_M, L_{CM} can be approximated as L_M, as expressed in Eq. (14). If the level of the DM noise at a frequency lower than the self-resonant frequency (SRF) of the CM choke is excessively high, the L_{DM}, i.e., L_k, is too small to attenuate the DM noise. Therefore, to suppress the DM noise using a high L_M, we propose a CM choke with an asymmetrical winding, in which the turns ratio of the primary and secondary windings of the CM choke are not equal. The non-identical turns ratio of the proposed CM choke cause the DM current to flow through L_M. Using Eqs. (8)–(11), Figs. 4 and 5 show the coupled and non-coupled models of the proposed CM choke at the CM and DM noise current flows.

By decoupling the original coupled model of the proposed CM choke and transforming the dual current sources into a single current source, we can derive the CM and DM noise impedances in the live and neutral lines, as shown in Figs. 4

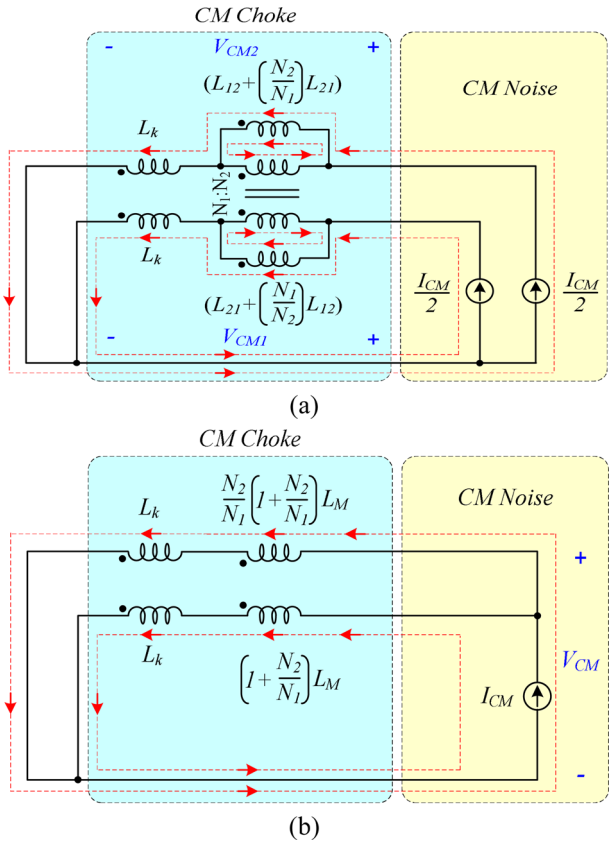

Fig. 4. Coupled and non-coupled model of the proposed CM choke at the CM noise current flow; (a) Coupled model, (b) Non-coupled model.

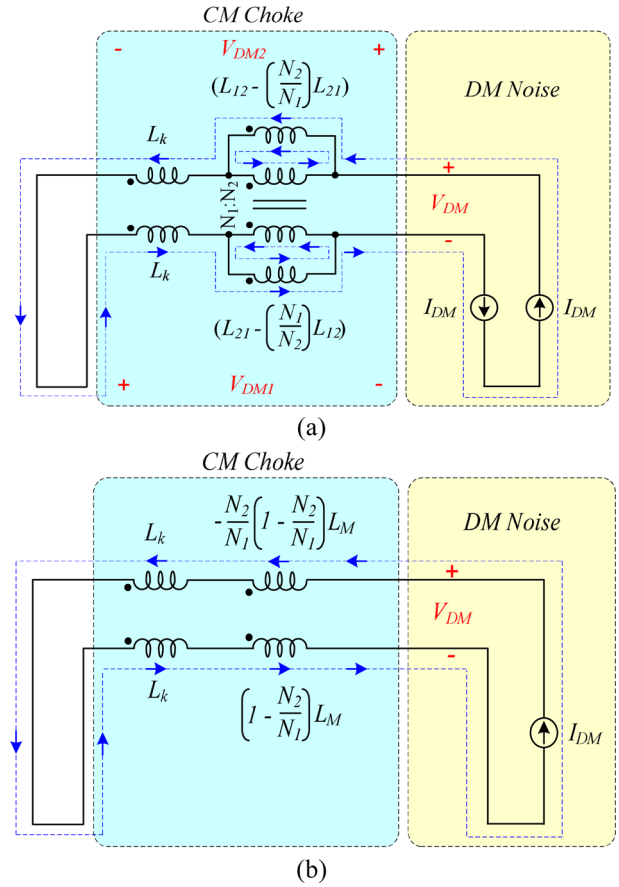

Fig. 5. Coupled and non-coupled model of the proposed CM choke at the DM noise current flow; (a) Coupled model, (b) Non-coupled model.

and 5, respectively. Therefore, as shown in Figs. 4 (b) and 5 (b), the CM and DM inductances (L_{CM} and L_{DM}) of the proposed CM choke with an asymmetrical windings can be derived using Eqs. (16) and (17), respectively, where L_k is assumed to be much smaller than L_M.

$$L_{CM} = \left(\left(1+\frac{N_2}{N_1}\right)L_M + L_k\right) \left\| \left(\frac{N_2}{N_1}\left(1+\frac{N_2}{N_1}\right)L_M + L_k\right) \right. \cong \frac{N_2}{N_1}L_M \tag{16}$$

$$L_{DM} = \left(1-\frac{N_2}{N_1}\right)L_M + L_k - \frac{N_2}{N_1}\left(1-\frac{N_2}{N_1}\right)L_M + L_k = \left(1-\frac{N_2}{N_1}\right)^2 L_M + 2L_k \tag{17}$$

Figs. 6 and 7 show the CM and DM impedances calculated using the simulation tool PSIM for the conventional and proposed CM chokes, where the parasitic capacitance and resistance are considered [19,20]. Practically, the parasitic impedances originating from the inter-winding capacitance effectively attenuate the EMI noise; however, the amount is negligible at low frequencies. Beyond a certain frequency, the effects of the parasitic elements begin to occur. This frequency is the dividing line between the "high frequency" and "low frequency" points. The effects of high frequencies include the permeability reduction of the CM choke core, the parasitic capacitance effect of the inductor, and the parasitic inductance effect of the filter capacitors. In addition to the effects of parasitic elements, radiation coupling and source impedance-filter capacitor resonance can also affect high-frequency EMI performance. These factors also affect the noise passing through the EMI filter [21]. However, these effects are beyond the scope of this paper.

As shown in Fig. 6, the CM impedance (Z_{CMP}) of the proposed CM choke with an asymmetrical winding is nearly equal to the CM impedance (Z_{CMC}) of a conventional choke. However, compared with the conventional DM impedance (Z_{DMC}), the proposed DM impedance (Z_{DMP}) is more than 40 times greater at low frequencies with the aid of L_M, as shown in Fig. 7. Therefore, the proposed CM choke with an asymmetrical winding can attenuate the DM noise more effectively than a conventional choke. The equivalent DM impedance of the proposed CM choke with an asymmetrical

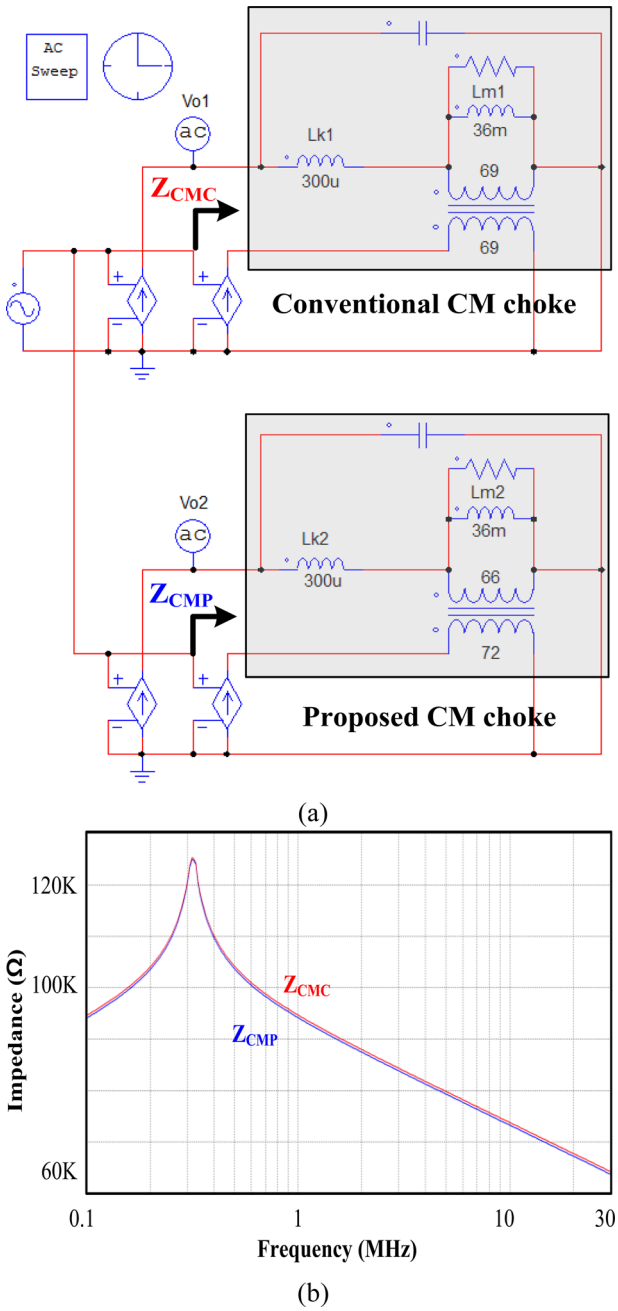

Fig. 6. CM impedances (Z_{CMC} and Z_{CMP}) of the conventional and proposed CM chokes calculated using PSIM simulation tool; (a) PSIM simulation circuit of Z_{CMC} and Z_{CMP}, (b) CM impedance characteristics of Z_{CMC} and Z_{CMP}.

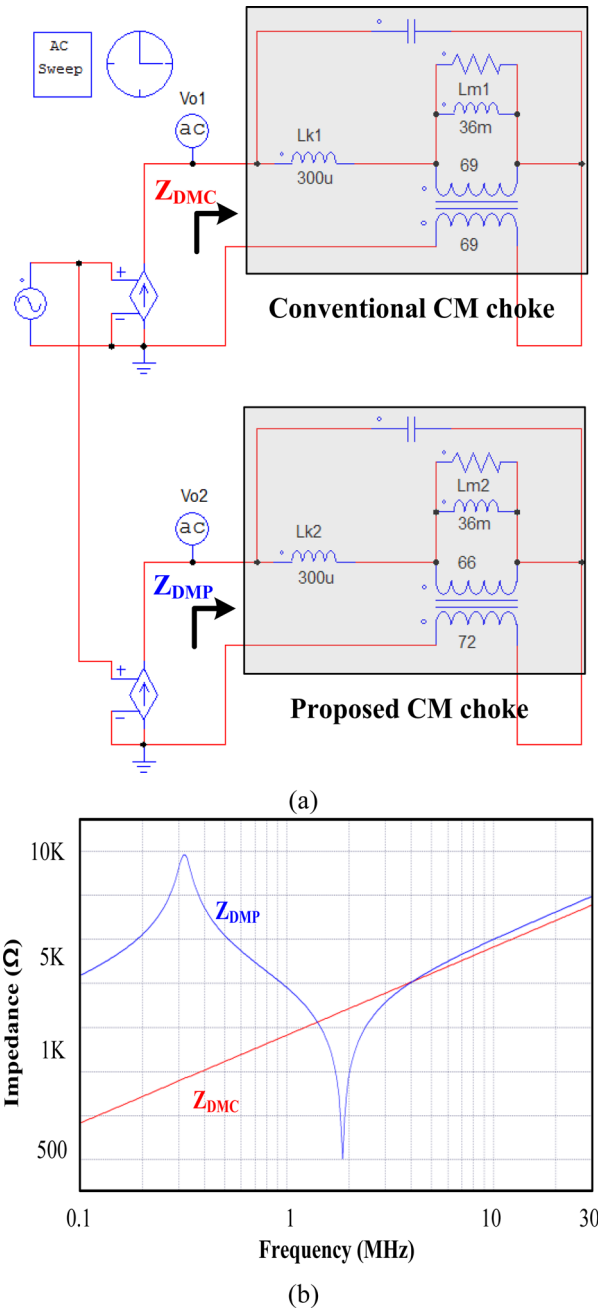

Fig. 7. DM impedances (Z_{DMC} and Z_{DMP}) of the conventional and proposed CM chokes calculated using PSIM; (a) PSIM simulation circuit of Z_{DMC} and Z_{DMP}, (b) CM impedance characteristics of Z_{DMC} and Z_{DMP}.

winding is very low at the second resonant frequency. Consequently, the DM noise cannot be attenuated. However, the low DM impedance at such frequencies is insignificant because the DM noise is often insignificant at high frequencies. If the DM noise at these frequencies is high, the proposed CM choke with an asymmetrical winding can achieve a high DM impedance by varying the turns ratio. Specifically, a high turns ratio of the proposed choke can increase the second resonant frequency.

3. DESIGN CONSIDERATION OF THE PROPOSED CM CHOKE WITH AN ASYMMETRICAL WINDING

The noise attenuation of an EMI filter must be analyzed prior to its design. However, the noise source and its source

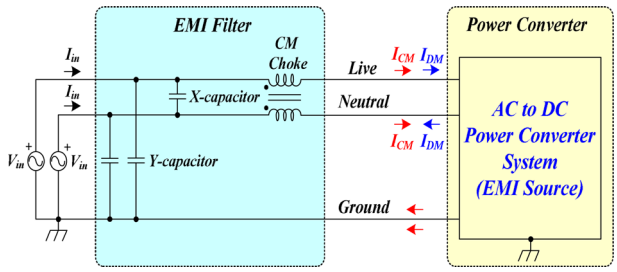

Fig. 8. Typical EMI filter configuration with its components and AC-to-DC power converter of the sensor power module (EMI source).

impedance can differ according to the printed circuit board (PCB) pattern, position of the EMI filter, type of the SMPS, and other factors. Therefore, the noise attenuation capability of the same EMI filter can differ depending on the SMPS [21]. From the design procedure proposed in an earlier study [22], the required CM and DM impedances (Z_{CM} and Z_{DM}) can be obtained from the required CM attenuation ($A_{CM,\,req}$), required DM attenuation ($A_{DM,\,req}$), and noise source impedances ($Z_{S,\,CM}$ and $Z_{S,\,DM}$), as shown in Eqs. (18) and (19).

$$Z_{CM} = (A_{CM,req} - 1)(25\Omega + Z_{S,CM}) \tag{18}$$

$$Z_{DM} = (A_{DM,req} - 1)(100\Omega + Z_{S,DM}) \tag{19}$$

where the values of $A_{CM,\,req}$, $A_{DM,\,req}$, $Z_{S,\,CM}$, and $Z_{S,\,DM}$ can be determined through measurements, and "25 Ω" and "100 Ω" denote the equivalent impedances of the line impedance stabilizing network (LISN) [22,23]. Therefore, L_{CM} and L_{DM} can be calculated from Eqs. (18) and (19).

Fig. 8 shows a commonly used EMI filter configuration with the components and an AC-to-DC power converter of the sensor power module (EMI source). Because the coupling capacitors between the "hot" and "cold" ground points act as Y-capacitors, the Y-capacitors may be placed only near the AC line [24]. Similarly, because a large input capacitor is used on the input side of the power converter, the X-capacitor can only be placed near the AC line.

If the EMI filter consists of only a CM choke without X-and Y-capacitors, the CM and DM inductances must be sufficiently large to attenuate each type of noise. However, because X- and Y-capacitors are typically used together with a CM choke, the CM and DM inductances can be designed to be smaller than those determined using Eqs. (18) and (19), respectively. Therefore, the CM and DM impedances (Z_{CM} and Z_{DM}), considering the existence of X- and Y-capacitors, can be recalculated using Eqs. (20) and (21).

$$Z_{CM} = (A_{CM,req} - 1)(25\Omega \| Z_Y/2 + Z_{S,CM}) \tag{20}$$

$$Z_{DM} = (A_{DM,req} - 1)(100\Omega \| (Z_X + 2Z_Y) + Z_{S,DM}) \tag{21}$$

where Z_X and Z_Y are the impedances of the X-and Y-capacitors, respectively. Moreover, because the Y-capacitors are used in live-to-ground and neutral-to-ground configurations, their impedance is divided by 2. To implement the choke with CM and DM inductances, as calculated using Eqs. (20) and (21), the number of turns should be determined by considering the core shape, size, material, and A_L-value. The number of primary turns can be derived using Eqs. (22) [25-27].

$$L_{CM} = A_L N_1^2 \tag{22}$$

where the A_L-value is the same as the permeance and is a measure of inductance in the magnetic cores. Eqs. (16) and (17) determine the number of turns on the secondary winding. The core saturation should be considered at the end of the design process. Because a large amount of the DM current does not flow through L_M, the conventional CM choke is rarely saturated. However, because the DM current of the proposed CM choke with an asymmetrical winding flows through L_M, core saturation must be considered. This is performed using Eq. (23).

$$B_{sat} = \mu(N_1 - N_2)I_{peak}/l_m \tag{23}$$

where μ, I_{peak}, and l_m represent the permeability of a magnetic

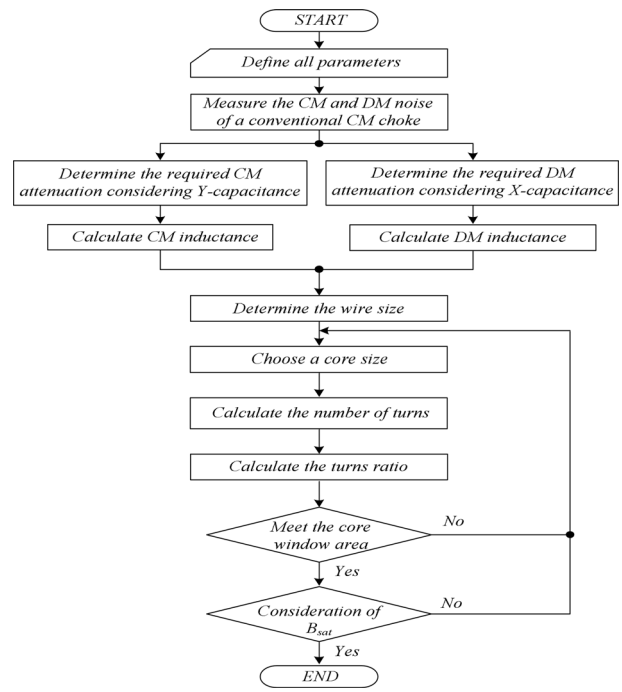

Fig. 9. Design flowchart of the proposed CM choke with an asymmetrical winding.

core, peak current flowing through the AC line, and mean path length of a magnetic core, respectively.

Based on the previous discussion, a flowchart [28-30] for designing the proposed CM choke with an asymmetrical winding is shown in Fig. 9. The first step is to measure the CM and DM noises of a conventional CM choke using a noise separator. As expressed in Eqs. (20) and (21), the second step is to determine the required CM attenuation, considering the Y-capacitance, and the required DM attenuation, considering the X-capacitance, using the CM and DM noise of a conventional CM choke obtained from the first step. The third step is to calculate the CM and DM inductances based on the data obtained in the second step. The fourth step is to determine the wire size [31,32] based on the nominal area of the wire (listed in the wire manufacturer's data sheets), winding fill factor, core window area, the number of turns between two windings, and peak winding current [25]. The fifth step is to select a core size that is sufficiently large to fit the turns of the wire gauge and satisfy the core's geometrical constant [31]. In the sixth step, the number of turns on the primary winding is calculated using Eq. (22). The seventh step calculates the turns ratio, which is the ratio of the number of turns between the primary and secondary windings, based on the sixth step. The eighth step is to determine whether the total winding area of the primary and secondary windings is included in the core window area. If the total winding area is not included in the core window area, the design process is repeated from the fifth stage to satisfy the design conditions. The final step determines whether the core is saturated using Eq. (23). If the core is saturated, the design process is repeated from the fifth step until the design condition is satisfied.

4. EXPERIMENTAL RESULTS AND DISCUSSION

Fig. 10 shows the 45-W flyback DC-to-DC converter implemented in the AC-to-DC power converter of the sensor power module. The design specifications of the input voltage (V_{in}), input maximum current ($I_{in\ max}$), output maximum current ($I_{o\ max}$) and output voltage (V_o) were V_{in} = 12 V, $I_{in\ max}$ = 0.2 A, $I_{o\ max}$ = 3.75 A, and V_o = 12 V, respectively. The EMI filter was composed of an X-capacitor (330 nF), two Y-capacitors (100 pF) and one CM choke. To adhere to the applicable regulations (CISPR 22-class B limit), we used a CM choke (TNC corporation-CV408360S, 36 mH, 69 turns) as the conventional filter. The leakage inductance of the conventional CM choke was approximately 300 μH.

Fig. 11 shows the test setup of the conducted EMI measurement used to measure the EMI noise in a practical AC-to-DC power converter of the sensor power module. In Fig. 11,

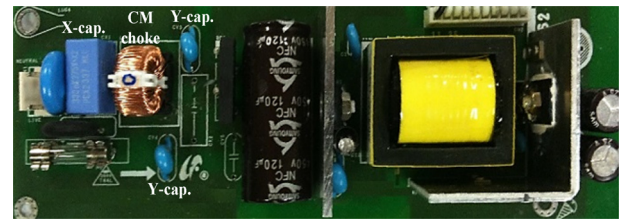

Fig. 10. 45-W flyback DC-to-DC converter implemented in an AC-to-DC power converter of the sensor power module.

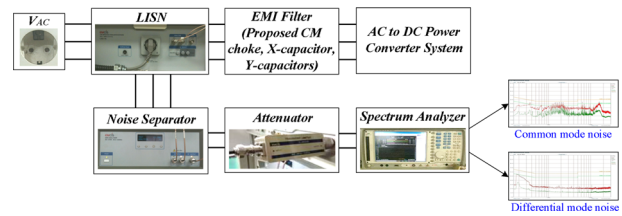

Fig. 11. Test setup of conducted EMI measurement for the proposed EMI filter in a practical AC-to-DC power converter of the sensor power module.

the CM and DM noises were measured using an LISN, a noise separator (EMCIS-EA 2100), an attenuator, and an Agilent 4395A spectrum analyzer. The noise separator was used to separate the CM and DM noises, and the spectrum analyzer was used to calculate the CM and DM noises from the other measured results. As shown in Fig. 11, an attenuator in the EMI equipment was used to reduce the strength of the EMI signal to prevent interference, such as the high-frequency surge current generated by the operation of electronic devices.

The measured result, as shown in Fig. 12 (b), indicated that the average DM noise margin of the conventional choke was as low as approximately 5 dB at 195 kHz. Because the tolerance of the component affects noise performance, a 10 dB margin for mass production is required. Therefore, a margin exceeding 5 dB must be added considering the DM noise. To satisfy these specifications with a conventional EMI filter, the leakage inductor of the CM choke must be larger, or an additional DM inductor must be used. In addition, for a design with a higher leakage inductance, a greater number of turns and a larger core are required. Fortunately, the CM noise has a sufficient margin at 195 kHz; hence, the designed CM inductance can be smaller than that of a conventional CM choke. Through Eqs. (20) and (21), Z_{CM} and Z_{DM} were derived again for the design of the proposed CM choke with an asymmetrical winding. The required CM and DM inductances were 33 mH and 550 μH, respectively. The minimum number of turns of the proposed CM choke with an asymmetrical winding can be calculated using the CM inductance. Given an A_L-value of 8.02 × 10^{-6} H/turns^2, this number was calculated as 66. With Eq. (17), the turns ratio of the proposed CM choke

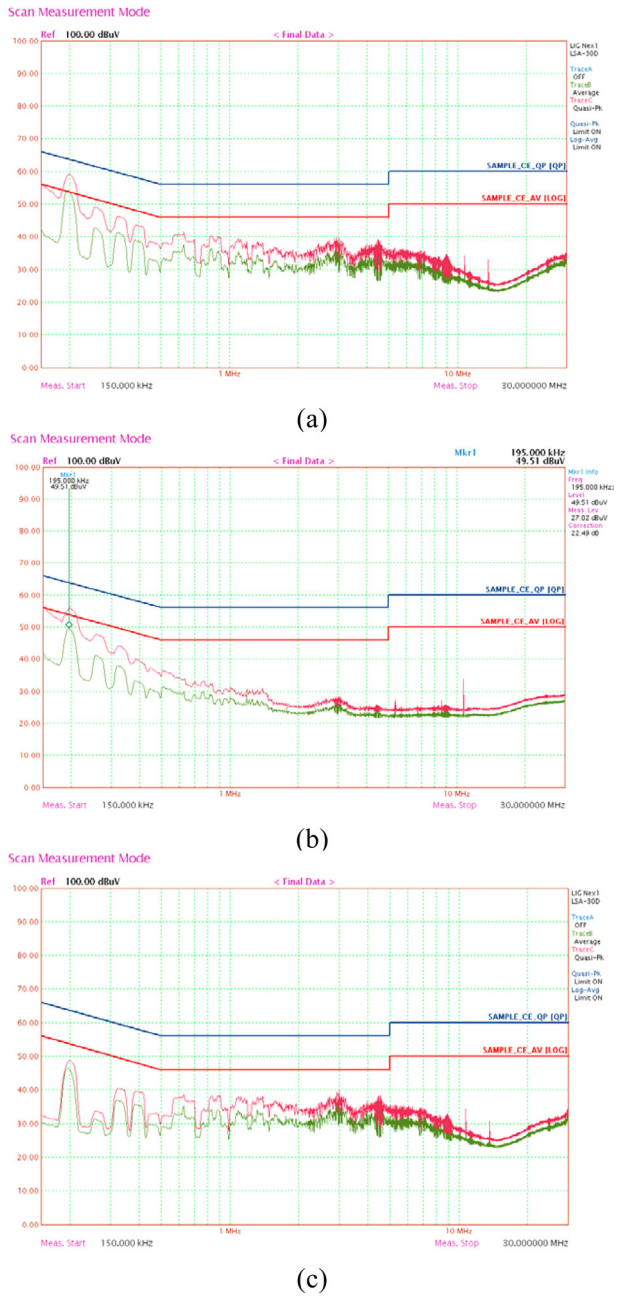

Fig. 12. Conducted EMI measurement results of a conventional CM choke; (a) Total noise of a conventional CM choke, (b) DM noise of a conventional CM choke, and (c) CM noise of a conventional CM choke.

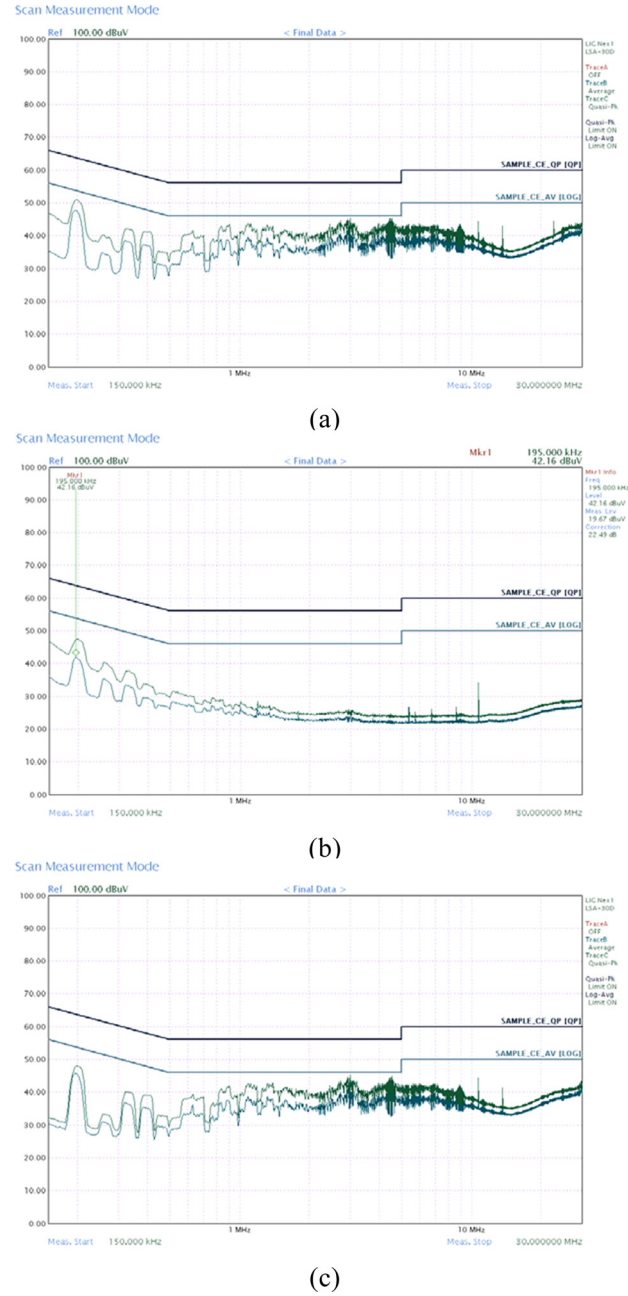

Fig. 13. Conducted EMI measurement results of the proposed CM choke with an asymmetrical winding; (a) Total noise of the proposed CM choke, (b) DM noise of the proposed CM choke, and (c) CM noise of the proposed CM choke.

with an asymmetrical winding can be derived, with the determined value here being 72:66.

As noted above, the saturation magnetic flux density of the proposed CM choke with an asymmetrical winding should be considered. As the magnetic flux density is proportional to the number of turns, input current, and permeability, the turns ratio is limited to the saturation magnetic flux density. Most manufacturing processes include data related to the maximum magnetic density of the core. With Eq. (23), the core cannot be saturated because the maximum magnetic flux density cannot exceed the saturation magnetic flux density. The measurement results comparing the conventional CM choke and proposed CM choke with an asymmetrical winding are shown in Figs. 12 and 13. The DM noise was suppressed to 43.5 dBμV at 195 KHz on the average measurement. Although the CM noise slightly increased, this amount was reasonable at high frequencies (up to 1 MHz). This was likely owing to the parasitic capacitance effect of the CM choke, the permeability reduction

effect of the core material for the CM choke, and the equivalent CM and DM inductance reduction effect of the non-coupled model of the proposed CM choke, among other factors. However, these effects were beyond the scope of this study.

5. CONCLUSIONS

A CM choke with an asymmetrical winding of the DM and CM noise suppression for low-power AC-to-DC power converters of sensor power modules is proposed in this paper. If the levels of CM and DM noise are high at frequencies below 1 MHz, CM and DM inductors must be used, requiring a larger filter and increased cost. The leakage inductance (L_k) of a CM choke must be larger than that of a conventional choke to ensure a satisfactory level of DM noise. For a design with a greater L_k, additional turns are required, and a larger core must be used. To use magnetizing inductance (L_M) to suppress DM noise, the proposed CM choke with an asymmetrical winding, where the turns ratio of the primary and secondary windings differ, was used in this study. With L_M, the DM noise of the AC-to-DC power converter of the sensor power module is significantly reduced. Although the CM noise slightly increased, the amount was within a reasonable range (up to 1 MHz). The proposed CM choke with an asymmetrical winding was experimentally verified as a simple and effective method to reduce the CM and DM noise in an AC-to-DC power converter of a sensor power module. Based on the experimental results and analysis in the present study, additional research is required to make this technology more practical. In future work, the winding method of the proposed CM choke with an asymmetrical winding for self-resonance frequency control will be studied.

CRediT Authorship Contribution Statement

Jong-Hae Kim: Investigation, Methodology, Writing - original draft. **Young-Woo Kim:** Conceptualization, Data curation. **Ku-Yong Kim:** Investigation, Methodology. **Jae-Sun Won:** Investigation, Methodology. **Do Kyung Lee:** Writing - review & editing, Supervision. **Young-Soo Sohn:** Writing - review & editing, Supervision.

Declaration of Competing Interest

The authors declare that they have no competing financial interests or personal relationships that may have influenced the work reported in this study.

Acknowledgements

This work was supported by research grants from Daegu Catholic University in 2025.

REFERENCES

[1] K. Mainali, R. Oruganti, Design of a Current-Sense Voltage-Feedback Common Mode EMI Filter for an Off-line Power Converter, Proceedings of 2008 IEEE Power Electron. Specialists Conf., Rhodes, Greece, 2008, pp. 1632–1638.
[2] L. Beghou, F. Costa, EMI-Based Current and Voltage sensing for the Control of Power Electronic Converters, IEEE Trans. Circuits Syst. II Express Briefs 65 (2018) 918–922.
[3] J. Palmer, S. Ji, X. Huang, L. Zhang, W. Giewont, F.F. Wang, et al., Improving Voltage Sensor Noise Immunity in a High Voltage and High dv/dt Environment, Proceedings of 2020 IEEE Appl. Power Electron. Conf. Exposition (APEC), New Orleans, USA, 2020, pp. 107–113.
[4] B. Narayanasamy, F. Luo, Y. Chu, Modeling and Stability Analysis of Voltage Sensing based Differential Mode Active EMI Filters for AC-DC Power Converters, Proceedings of 2018 IEEE Symp. Electromagn. Compat., Signal Integr. Power Integr. (EMC, SI & PI), Long Beach, USA, 2018, pp. 322–328.
[5] K. Kostov, V. Tuomainen, J. Kyyrä, T. Suntio, Designing Power Line Filters for DC-DC Converters, Proceedings of the 11th Int. Power Electron. Motion Control Conf. (EPE-PEMC 2004), Riga, Latvia, 2004.
[6] K. Kostov, A. Niinikoski, J. Kyyra, T. Suntio, Prediction of the conducted EMI from DC-DC switched-mode power converters, Proceedings of the 11th Int. Power Electron. Motion Control Conf. (EPE-PEMC 2004), Riga, Latvia, 2004.
[7] D. Nemashkalo, N. Moonen, F. Leferink, Practical Consideration on Power Line Filter Design and Implementation, Proceedings of 2020 Int. Symp. Electromagn. Compat. EMC EUROPE, Rome, Italy, 2020, pp. 23–25.
[8] K. Fu, W. Chen, S. Lin, A General Transformer Evaluation Method for Common-Mode Noise Behavior, Energies 12 (2019) 1984.
[9] S. Khelladi, K. Saci, A. Hadjadj, A. Ales, A Hybrid Common Mode Choke Optimization Method for Input Line EMI Filter Design, Adv. Electromagn. 10 (2021) 56–66.
[10] C.R. Paul, Introduction to Electromagnetic Compatibility, 2nd ed., John Wiley & Sons, Hoboken, 2006, pp. 377–416.
[11] S. Maniktala, Switching Power Supplies A to Z, 1st ed., Newnes, Boston, USA, 2006, pp. 373–386.
[12] H.S. Kim, S.K. Han, J.S. Won, J.C. Ju, D.J. Lee, D.S. Oh, et al., A new asymmetrical winding common mode choke capable of attenuating differential mode noise, Proceedings of 8th Int. Conf. Power Electron. ECCE Asia, Jeju, Korea (South), 2011, pp. 440–445.
[13] R. Lai, Y. Maillet, F. Wang, S. Wang, R. Burgos, D. Boroyevich, An Integrated EMI Choke for Differential-Mode and Common-Mode Noise Suppression, IEEE Trans. Power Electron. 25 (2010) 539–544.
[14] L. Dai, W. Chen, X. Yang, M. Zheng, Y. Yang, R. Wang, A Multi-Function Common Mode Choke Based on Active CM EMI Filters for AC/DC Power Converters, IEEE Access 7 (2019) 43534–43546.
[15] F.A. Kharanaq, A. Emadi, B. Bilgin, Modeling of Con-

ducted Emissions for EMI Analysis of Power Converters: State-of-the-Art Review, IEEE Access, 8 (2020) 189313–189325.
[16] K. Kostov, J. Kyyra, Common-Mode Choke Coils Characterization, Proceedings of 2009 13th Eur. Conf. Power Electron. Appl., Barcelona, Spain, 2009.
[17] W. G. Hurley, D. J. Wilcox, Calculation of Leakage Inductance in Transformer Windings, IEEE Trans. Power Electron. 9 (1994) 121–126.
[18] H.J. Jung, S. Yoon, Y.S. Kim, S. Bae, Y.S. Lim, Method of High-Frequency Modeling of Common-Mode Choke, J. Korean Inst. Electromagn. Eng. Sci. 28 (2017) 964–973.
[19] S. Wang, F.C. Lee, J.D. Van Wyk, Design of Inductor Winding Capacitance Cancellation for EMI Suppression, IEEE Trans. Power Electron. 21 (2006) 1825–1832.
[20] S.-P. Weber, E. Hoene, S. Guttowski, W. John, H. Reichl, On Coupling with EMI Capacitors, Proceedings of 2004 Int. Symp. Electromagn. Compat., Silicon Valley, USA, 2004.
[21] F.Y. Shih, D.Y. Chen, Y.P. Wu, Y.T. Chen, A procedure for designing EMI filters for AC line applications, IEEE Trans. Power Electron. 11 (1996) 170–181.
[22] D. Zhang, D.Y. Chen, M.J. Nave, D. Sable, Measurement of noise source impedance of off-line converters, IEEE Trans. Power Electron. 15 (2000) 820–825.
[23] M.J. Nave, Power Line Filter Design for Switched Mode Power Supplies, 2nd ed., Van Nostrand Reinhold, New York, 1991, pp. 29–113.
[24] H.W. Ott, Noise Reduction Techniques in Electronic Systems, 2nd ed., Wiley, New York, 1998, pp. 137–158.
[25] A.I. Pressman, K.H. Billings, T. Morey, Switching Power Supply Design, 3rd ed., McGraw-Hill, New York, 2009, pp. 267–276.
[26] R. West, Common Mode Inductors for EMI Filters Require Careful Attention to Core Material Selection, Power conversion Intell. Motion-Eng. Ed. 21 (1995) 52–59.
[27] Y. Maillet, R. Lai, S. Wang, F. Wang, R. Burgos, D. Boroyevich, High-Density EMI Filter Design for DC-Fed Motor Drives, IEEE Trans. Power Electron. 25 (2010) 1163–1172.
[28] I. Cadirci, B. Saka, Y. Eristiren, Practical EM filter design procedure for high-power high-frequency SMPS according to MIL-STD 461, IEE Proc. Electr. Power Appl. 152 (2005) 775–782.
[29] J. Jiraprasertwong, C. Jettanasen, Practical Design of a Passive EMI Filter for Reduction of EMI Generation, Proceedings of Int. Multi Conf. Eng. Comput. Scientists 2015 Vol II, Hong Kong, 2015, pp. 639–642.
[30] A. Raj.N, O.M.S. Chandrachood, A.K. Prakash, K.K. Mukundan, A Study on Conducted Emission from Switching Power Converters and a Systematic Design Procedure for EMI Filters, Int. J. Adv. Res. Electr. Electron. Instrum. Eng. 3 (2014) 7616–7623.
[31] R.W. Erickson, D. Maksimovic, Fundamental of Power Electronics, 3rd ed., Springer, New York, 2020, pp. 539–584.
[32] C.-T. Phan-Tan, T. Ngo-Phi, N. Nguyen-Quang, Design Procedure and Implementation of Inductor Using Litz Wires for Induction Heating, Proceeding of 2023 Int. Conf. Syst. Sci. Eng. (ICSSE), Ho Chi Minh, Vietnam, 2023, pp. 370–374.